Computational studies of the potential energy surface for $O(^3P)+H_2S$: Characterization of transition states and the enthalpy of formation of HSO and HOS

A. Goumri, Dianna Laakso, John-David R. Rocha, C. E. Smith, and Paul Marshall
Department of Chemistry, University of North Texas P.O. Box 5068, Denton, Texas 76203-5068

(Received 5 August 1994; accepted 28 September 1994)

Structures and vibrational frequencies for minima and 11 transition states on the $O(^3P)+H_2S$ potential energy surface have been characterized at the MP2=FULL/6-31G(d) level. GAUSSIAN-2 theory was employed to calculate $\Delta H_{f,298}$ for HSO and HOS of -19.9 and -5.5 kJ mol^{-1}, respectively. The kinetics of HSO⇌HOS isomerization are analyzed by Rice–Ramsperger–Kassel–Marcus theory. Transition state theory analysis for $O+H_2S$ suggests OH+HS is the dominant product channel, with a rate constant given by 1.24×10^{-16} $(T/\mathrm{K})^{1.746}\exp(-1457\ \mathrm{K}/T)$ cm^3 molecule^{-1} s^{-1}. Kinetic isotope effects and the branching ratio for H+HSO production are also analyzed. The other possible products H_2+SO and H_2O+S do not appear to be formed in single elementary steps, but low-barrier pathways to these species via secondary reactions are identified. No bound adducts of $O+H_2S$ were found, but results for weakly bound triplet HOSH are presented. The likely kinetics for the reactions $OH+SH\rightarrow S(^3P)+H_2O$, OH+SH→*cis* and *trans* ^{3}HOSH, *cis* ^{3}HOSH→HOS+H, and HSO and HOS+H→$H_2+{}^3$SO are discussed. © *1995 American Institute of Physics.*

I. INTRODUCTION

The reaction of ground state oxygen atoms with hydrogen sulfide is included in flame models[1] and in kinetic compilations focused on atmospheric chemistry,[2,3] but considerable uncertainty remains in the temperature dependence of the thermal rate constant, k_1, and the branching ratios for the various possible product channels which are all spin allowed

$$O(^3P)+H_2S\rightarrow OH+SH \quad (1a)$$

$$\rightarrow HSO+H \quad (1b)$$

$$\rightarrow H_2+SO \quad (1c)$$

$$\rightarrow HOS+H. \quad (1d)$$

There have been several laboratory studies of reactions (1) in thermally equilibrated systems,[4–13] which have been reviewed elsewhere.[14,15] The latest recommendations are that Eq. (1a) is the dominant pathway[15] and that the overall rate constant k_1 is $1.4\times10^{-11}\exp(-16.0\pm6.2\ \mathrm{kJ\,mol^{-1}/RT})$ cm^3 molecule^{-1} s^{-1} for 290–500 K.[3] Data obtained above about 1000 K (Refs. 4 and 5) lie above an extrapolation of this Arrhenius expression while the data of Hollinden *et al.*[9] showed smaller values of the pre-exponential factor, A, and activation energy, E_a, below room temperature, which might indicate a change of mechanism there. Reaction (1b) leading to HSO was discussed by Slagle *et al.*[12] and Singleton *et al.*,[13] although Whytock *et al.*[11] argued in favor of Eq. (1a) based on the kinetic isotope effect. The most recent measurements on the branching ratio were by Singleton *et al.*[16] who concluded $k_{1b}/k_1<0.2$ at room temperature. Some authors considered Eq. (1b) to be an addition pathway, with initial formation of an excited adduct which then decomposes, a view supported by the matrix-isolation experiments of $O(^3P)+H_2S$ by Smardzewski and Lin[17] who observed formation of HOSH. The pathway to H_2+SO was proposed by Bradley and Dobson[18] and Frenklach *et al.*[1] to explain their high-temperature observations; the E_a for Eq. (1c) appears to be much higher than for Eq. (1a), around 33–40 kJ mol^{-1}, so that Eq. (1c) can only be a minor channel. The possibility of channel (1d) was raised by White and Gardiner[19] because of the potentially greater stability of HOS as compared to HSO.

Single collisions between $O(^3P)+H_2S$ have been analyzed in molecular beam experiments,[20–22] which revealed formation of HSO (or HOS) at a threshold translational energy similar to the overall E_a of reaction (1). Davidson *et al.*[20] interpreted their results to imply $\Delta H_{f,0}(\mathrm{HSO})=-6\pm8$ kJ mol^{-1}, and Balucani *et al.*[22] obtained -3.7 ± 2.9 kJ mol^{-1} for this quantity. The stability of HSO is important both for understanding the chemistry of sulfur in flames[1] and in the atmosphere,[23] where HSO is likely to be an important intermediate. In particular, the feasibility of the atmospheric cycle[24]

$$HS+O_3\rightarrow HSO+O_2, \quad (2a)$$

$$HSO+O_3\rightarrow HS+2O_2 \quad (2b)$$

depends on the possible exothermicity of reaction (2b). There have been numerous experimental and theoretical studies of the HSO and HOS isomers,[25–44] and previous thermochemical data for HSO and HOS are summarized in Table I (thermochemical data are quoted to one decimal place to avoid rounding errors without implication of this degree of accuracy). There is a wide variation, of over 80 kJ mol^{-1}, in $\Delta H_{f,298}$(HSO) and a wider spread in the estimated stabilities of HOS versus HSO, even though systematic errors might have been expected to cancel for the latter quantity.

There are also two *ab initio* studies that addressed transition states for reactions (1a) and (1b). The first by Zhu *et al.*[45] characterized a pathway leading to HSO+H; at the MP2/6-311G(d,p) level of theory they employed, we find that the classical barrier height is 168 kJ mol^{-1}. Takane and

TABLE I. Comparison of thermochemical results for HSO and HOS, in kJ mol^{-1}.

$\Delta H_{f,298}$(HSO)	$\Delta H_{f,298}$(HOS)	$\Delta H_{f,298}$(HSO)-$\Delta H_{f,298}$(HOS)	Method	Ref.
≤62.3	⋯	⋯	$HS+O_3$ chemiluminescence	25
⋯	⋯	50.2	*Ab initio*	27
<11.3, ≈−12.6	⋯	⋯	$O+H_2S$ kinetics	12
51.5±16.7	⋯	⋯	Re-evaluation of Ref. 25	19
−20.9±16.7	20.9±16.7	−41.8±23.6	Bond additivity	28
⋯	⋯	41.0	*Ab initio*	29
−8.9± 8.0[a]	⋯	⋯	$O+H_2S$ molecular beam	20
⋯	⋯	40.6	*Ab initio*	33
−1.7±12.6	−12.1±12.6	10.5± 8.4	*Ab initio*	35
⋯	⋯	19.7	*Ab initio*	36
−25.5± 5.4	−2.9± 5.4	−22.6± 0.8	*Ab initio*	37
−6.7± 2.9[a]	⋯	⋯	$O+H_2S$ molecular beam	22
⋯	−2.1± 8.4	⋯	Kinetics of HOS^-	38
−4.8± 7.3	−20.9 ± 8.8	16.1 ± 11.4	*Ab initio*	39
−11.7± 3.8[a]	⋯	⋯	*Ab initio*	41
⋯	⋯	27.2	*Ab initio*	43
−20.5± 5.4	−10.0	−10.5	*Ab initio*	44
−19.9	−5.5	−14.4	*Ab initio*	This work

[a]Data for 0 K converted to 298 K by subtraction of 2.9 and 2.8 kJ mol^{-1} for HSO and HOS (see the text).

Fueno[46] analyzed two other transition states, and with CI(full)/Ryd theory obtained classical barriers of 77 and 127 kJ mol^{-1} for abstraction and displacement, respectively. All these theoretical barriers imply rate constants 10 or more orders of magnitude smaller than observed at room temperature.

In an effort to resolve some of the discrepancies noted above, we have made a fairly comprehensive study of the triplet $O+H_2S$ potential energy surface (PES) at a uniform and high level of *ab initio* theory. We employ the GAUSSIAN-2 (G2) methodology, which has a target accuracy of ±8 kJ mol^{-1} for atomization enthalpies and an average absolute deviation of 5 kJ mol^{-1},[47–49] to obtain approximate QCISD(T)/6-311+G(3df,2p) energies. As shown below, this level of computation yields excellent accord with the thermochemistry where it is well established, including the latest information for HOS. Our PES provides a context for possible reinterpretation of experimental data for HSO and a resolution between the latest computational and molecular beam estimates of $\Delta H_{f,298}$(HSO). Transition states are analyzed and the results used to predict the rate constants and kinetic isotope effects *ab initio* for the first time, for comparison with experiment.

II. *AB INITIO* METHODOLOGY

The general principles of quantitative molecular orbital theory have been described elsewhere,[50,51] and the *ab initio* calculations were carried out with the GAUSSIAN90 and 92 programs.[52,53] Preliminary searches of the triplet PES were made at the self-consistent field or Hartree–Fock (HF) and second-order Møller–Plesset (MP2) levels of theory with the 3-21G(d) and 6-31G(d) basis sets and spin-unrestricted wave functions. The MP2 calculations incorporate a partial correction for the effects of electron correlation. Each stationary point was characterized as a true minimum (all vibrational frequencies real) or a transition state (a single imaginary frequency) at the MP2=FULL/6-31G(d) level. The reactants and products connected by each transition state (TS) were confirmed by visualization of the imaginary vibrational normal mode and/or by following the intrinsic reaction coordinate. The calculated harmonic frequencies were scaled by a standard factor of 0.95 to account for effects of basis set deficiency and anharmonicity, and are used to derive the zero-point vibrational energy ΔE(ZPE) and various thermodynamic quantities. The stability of the wave function with respect to relaxation of internal constraints[54] was verified at each stationary point.

The next step was to obtain the energy at each stationary point, at a much higher level of theory. Approximate QCISD(T)/6-311+G(3df,2p) energies were calculated at the MP2=FULL/6-31G(d) geometries by means of the G2 methodology.[49] Briefly, the MP4/6-311G(d,p) energy was modified with a series of additive corrections defined as follows: $\Delta E(+)=E$[MP4/6-311+G(d,p)]$-E$(MP4/6-311G(d,p)], $\Delta E(2df)=E$[MP4/6-311G(2df,p)]$-E$(MP4/6-311G(d,p)], ΔE(QCI)=E[QCISD(T)/6-311G(d,p)] $-E$(MP4/6-311G(d,p)], and ΔE(HLC)=(−0.000 19 n_{unpair}−0.00614 n_{pair}) a.u. (1 a.u.≈2625 kJ mol^{-1}), where n_{unpair} and n_{pair} represent the numbers of unpaired valence electrons and valence pairs, respectively. The G1 energy is defined as E(G1)=E[MP4/6-311G(d,p)]+$\Delta E(+)$ +$\Delta E(2df)+\Delta E$(QCI)+ΔE(HLC)+ΔE(ZPE). The further term $\Delta=E$[MP2/6-311+G(3df,2p)]$-E$(MP2/6-311G(2df,p) − E(MP2/6-311+G(d,p)] + E(MP2/6-311G(d,p)] leads to the G2 energy as E(G2)=E(G1)+Δ +0.001 14 n_{pair} a.u. Our use of MP2 rather than HF frequencies to obtain ΔE(ZPE) is a modification of the original G2 method; we have summarized the small changes in energy for the published G2 energies of relevant one-, two-, and three-atom species elsewhere.[55]

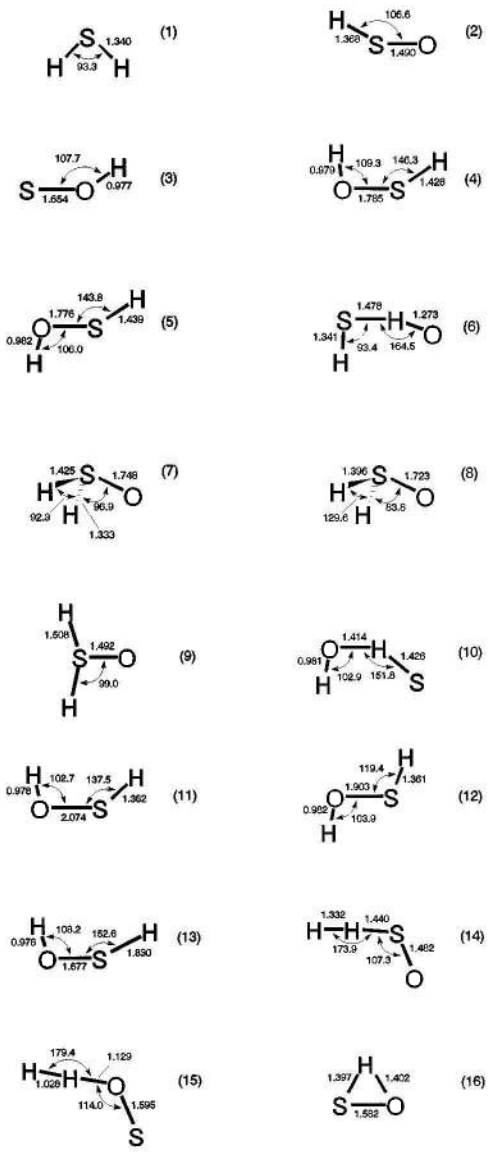

FIG. 1. MP2=FULL/6-31G(d) geometries for bound minima and transition states on the triplet $O+H_2S$ PES: (1) H_2S, (2) HSO, (3) HOS, (4) *cis* HOSH, (5) *trans* HOSH, (6) TS1, (7) TS2, (8) TS3, (9) TS4, (10) TS5, (11) TS6, (12) TS7, (13) TS8, (14) TS9, (15) TS10, (16) TS11. Distances in Å and angles in degrees.

III. RESULTS AND DISCUSSION

A. Geometries and vibrational frequencies

Figure 1 shows MP2=FULL/6-31G(d) geometries for bound minima and transition states for the following processes:

$$\text{TS1: } O(^3P)+H_2S\rightarrow OH+SH, \tag{1a}$$

$$\text{TS2: } O(^3P)+H_2S\rightarrow HSO+H, \tag{1b}$$

$$\text{TS3: } O(^3P)+H_2S\rightarrow TS4, \tag{3}$$

$$\text{TS4: } TS3\rightarrow HSO+H, \tag{4}$$

$$\text{TS5: } OH+SH\rightarrow S(^3P)+H_2O, \tag{5}$$

$$\text{TS6: } OH+SH\rightarrow cis\text{-}^3HOSH, \tag{6}$$

$$\text{TS7: } OH+SH\rightarrow trans\text{-}^3HOSH, \tag{7}$$

$$\text{TS8: } cis\text{-}^3HOSH\rightarrow HOS+H, \tag{8}$$

$$\text{TS9: } HSO+H\rightarrow H_2+{}^3SO, \tag{9}$$

$$\text{TS10: } HOS+H\rightarrow H_2+{}^3SO, \tag{10}$$

$$\text{TS11: } HSO\rightarrow HOS. \tag{11}$$

The scaled MP2=FULL/6-31G(d) vibrational frequencies are summarized in Table II. We can compare our results for HSO with experimental quantities, but only those actually measured rather than inferred, e.g., by means of Badger's rule. Rotationally resolved LIF spectra of HSO and DSO yielded[32] H–S and S–O distances of 1.389 ± 0.005 and 1.494 ± 0.005 Å, respectively, and an angle of $106.6°\pm0.5°$ which, as noted by Chang and Loew,[40] are extremely near to the MP2=FULL/6-31G(d) values. There is similar accord for MP2/DZP results,[43] and CASSCF+1+2 data[37] are almost as close. The MP2/6-31G(d) S–O distance lies between those known for SO_2 (1.43 Å)[56] and H_2SO_4 (1.57 Å),[57] and suggests some multiple bond character. The spin densities derived from the HF/6-311+G($3df,2p$) wave function are 0.43 on S and 0.60 on O, suggesting that the unpaired electron density is spread across S and O. The dipole moment with this wave function is 2.27 D (1 D$\approx3.336\times10^{-29}$ C m). Our MP2=FULL/6-31G(d) and previous MP2=FULL/DZP[43] data somewhat overestimate the S–O stretching frequency measured at 1013 or 1009 cm^{-1} (Refs. 25 and 34, respectively), while the CASSCF+1+2[37] result is very close. The S–H stretch has not been observed directly; our value of 2418 cm^{-1} lies between two empirical estimates.[25,32] The bending mode has only been observed in DSO,[25] at 770 cm^{-1} cf. the MP2/6-31G(d) estimate of 767 cm^{-1},[58] so the estimate for HSO of 1017 cm^{-1} should be reliable.

There are no measured geometries or frequencies for other bound minima, although for HOS there is good accord with two recent computational investigations.[37,43] The S–O bond length is greater than in HSO, suggestive of simple σ bonding between S and O, and the unpaired electron is localized on the S atom as revealed by the spin density there of 0.96. The dipole moment is predicted to be 1.58 D. Singlet HOSH is well known,[59] but a novel triplet adduct of OH and HS, with bound *cis* and *trans* HOSH isomers, is proposed. The dipole moments are predicted to be 2.03 and 1.37 D, respectively, from the HF/6-311+G($3df,2p$) wave function, and both isomers have similar spin densities of about 1.4 on S and about 0.3–0.4 on O. We point out that the MP2=FULL/6-3G(d) calculations have probably underestimated the already large S–O separation, based on the G2 results discussed below.

These minima and the transition states TS1–TS11 connect as shown on Fig. 2, where total energies, that exclude ZPE, are plotted. This is the PES that was searched at the MP2=FULL/6-31G(d) level. It may be seen that the chemistry of the triplet O/H/H/S system is dominated by bimolecular processes, by contrast to the singlet PES.[59] We made special efforts to locate bound triplet $O+H_2S$ adducts which have been proposed as possible reaction intermediates, but

TABLE II. Scaled MP2=FULL/6-31G(d) frequencies, in cm^{-1}, for stationary points on the $O(^3P)+H_2S$ PES.

HSO		HOS		*cis* ^{3}HOSH		*trans* ^{3}HOSH		TS1		TS2		TS3		TS4	
Sym.	ν	Sym.	ν	Sym.	ν	Sym.	ν	Sym.	ν	Sym.	ν	Sym.	ν	Sym.	ν
A'	1017	A'	828	A'	547	A'	561	A'	2407i	A	410i	A'	791i	$B2$	1016i
A'	1170	A'	1180	A''	599	A''	590	A'	242	A	369	A''	380	$A1$	769
A'	2418	A'	3521	A'	766	A'	786	A''	414	A	670	A'	686	$B1$	838
				A'	986	A'	1002	A'	580	A	1234	A'	1000	$B2$	914
				A'	1966	A'	1825	A'	1017	A	1877	A''	1944	$A1$	1131
				A'	3521	A'	3469	A'	2660	A	2710	A'	2043	$A1$	1613

TS5		TS6		TS7		TS8		TS9		TS10		TS11	
Sym.	ν	Sym.	ν	Sym.	ν	Sym.	ν	Sym.	ν	Sym.	ν	Sym.	ν
A'	1397i	A'	313i	A'	611i	A'	923i	A'	1306i	A'	2383i	A'	2947i
A'	219	A''	319	A''	429	A'	486	A'	216	A'	313	A'	1013
A''	293	A'	447	A'	473	A''	572	A''	612	A''	601	A'	2489
A'	748	A'	824	A'	793	A'	812	A'	1101	A'	868		
A'	1299	A'	2494	A'	2471	A'	1124	A'	1219	A'	964		
A'	3536	A'	3550	A'	3475	A'	3517	A'	1359	A'	1045		

none were found at up to the MP2=FULL/6-31G(d) level of theory. We also made single point MP2/6-31+G(2d) calculations at likely planar and pyramidal geometries for ^3H_2SO, but the energies were more positive than for separated O and H_2S.

B. Thermochemistry

Bound minima on the triplet PES were examined in greater detail, and components of the G2 energies are listed in Table III. The quantities n_{pair} and n_{unpair} (see Sec. II) are conserved in calculations of relative enthalpies, H_{rel}, and thus the empirical HLC component of the G2 method cancels out. The expectation values of S^2 are close to the ideal values of 0.75 and 2 for doublet and triplet species, so spin contamination will not have a large effect on the G2 energies. These energies yield heats of formation for unknown minima via the hydrogenation reaction

$$\text{minimum (g)}+H_2(g)\rightarrow H_2O(g)+H_2S(g) \qquad (12)$$

for which the change in G2 energy equals the enthalpy change at 0 K, ΔH_0. Because by definition the G2 method gives the correct H_2 dissociation energy, reaction (12) is identically equivalent to isogyric reactions where H atoms are added to or subtracted from each side. For this kind of process, errors arising from inadequate basis sets or incomplete accounting for electron correlation largely cancel, as does any basis set superposition error.[60] $\Delta H_{f,0}$(minimum) is obtained from ΔH_0 and the measured $\Delta H_{f,0}$ of H_2O and H_2S.[56]

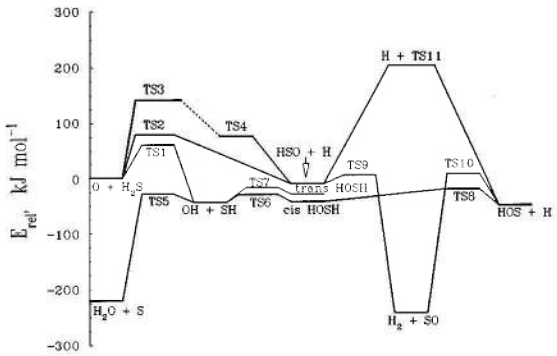

FIG. 2. Potential energy surface calculated at the MP2=FULL/6-31G(d) level, showing energies (excluding ZPE) relative to $O(^3P)+H_2S$.

Table IV shows the results of this approach for $\Delta H_{f,0}$ of various known minima, taken from the JANAF Tables[56] except for HS where we employ the measurement by Nicovich *et al.*[61] that is consistent with other recent determinations.[62,63] There is excellent accord with the experimental $\Delta H_{f,0}$ for $O+H_2S$, $OH+SH$, H_2O+S, H_2+SO, and HOS+H where the worst error is less than 5 kJ mol^{-1}. Assignment of precise quantitative error limits to the G2 thermochemistry is hard; given the performance here and in the initial set of test molecules[49] an uncertainty of 5–10 kJ mol^{-1} seems reasonable. Use of Eq. (12) leads to $\Delta H_{f,0}$ for HOS and HSO of -2.7 and -17.0 kJ mol^{-1}, respectively. Other thermochemical properties for 200–2000 K are derived via statistical mechanics[64] and listed in Tables V and VI. No previous tabulation for HOS has apparently been published, and our data supersede those of White and Gardiner[19] because the ΔH_f of HSO employed here is more accurate. Our ΔH_f for HSO is in accord with upper limits derived from H_2S+O kinetic studies and observations of chemiluminescence from $HS+O_3$ (see Table I), and is within the limits of the combined uncertainty when compared with the molecular beam experiments of Davidson *et al.*[20] The discrepancy with the molecular beam result of Balucani *et al.*[22] is probably significant. They obtained ΔH_0 for reaction (1b) through consideration of the difference between the energies of the products and the energy of collisions between $O(^3P)$ and H_2S with essentially zero internal energy. The energy of the products was taken to be equal to the maximum energy release into translation of HSO, E_{tot}. However, it might be that, given the significant barrier to this process and especially if the PES is "attractive" with a barrier early

TABLE III. Absolute G2 energies of stationary points on the $O(^3P)+H_2S$ PES calculated at the MP2=FULL/6-31G(d) optimized geometries.

Species	Sym.	State	MP4/6-311G(d,p)[a]	$\langle S^2\rangle$[b]	$\Delta E(+)$[c]	$\Delta E(2df)$[c]	ΔE(QCI)[c]	ΔE(ZPE)[c]	Δ[c]	E(G2)[a]	H_{rel}^d
HSO	C_s	$^2A''$	−473.278 37	0.766	−10.14	−101.13	−3.41	10.49	−10.35	−473.423 10	−27.8[e]
HOS	C_s	$^2A''$	−473.288 17	0.761	−9.74	−93.35	−0.76	12.59	−8.05	−474.417 68	−13.6[e]
cis HOSH	C_s	$^3A''$	−473.806 98	2.035	−10.38	−91.47	−4.73	19.10	−11.70	−473.936 54	−63.1
trans HOSH	C_s	$^3A''$	−473.799 54	2.031	−12.75	−92.64	−3.81	18.75	−11.09	−473.931 46	−49.7
TS1	C_s	$^3A''$	−473.782 36	2.057	−7.40	−79.60	−5.96	11.19	−9.08	−473.903 59	+23.4
TS2	C_1	^3A	−473.766 75	2.060	−8.26	−92.44	−8.28	15.63	−11.41	−473.901 89	+27.9
TS3	C_s	$^3A'$	−473.739 42	2.033	−11.09	−95.14	+4.41	13.79	−10.47	−473.868 30	+116.1
TS4	C_{2v}	$^3B_1$	−473.759 88	2.062	−10.01	−104.97	−5.01	11.99	−11.58	−473.909 84	+7.0
TS5	C_s	$^3A''$	−473.810 97	2.035	−9.39	−81.48	−5.92	13.88	−9.42	−473.933 68	−55.6
TS6	C_s	$^3A''$	−473.808 75	2.061	−11.40	−84.64	−11.24	17.39	−10.35	−473.939 37	−70.5
TS7	C_s	$^3A''$	−473.799 43	2.029	−14.34	−89.67	−8.50	17.41	−10.90	−473.935 81	−61.2
TS8	C_s	$^3A''$	−473.788 13	2.061	−9.04	−94.21	−4.55	14.83	−10.46	−473.921 94	−24.8
TS9	C_s	$^3A''$	−473.775 85	2.047	−10.26	−101.09	−5.49	10.26	−10.82	−473.923 63	−29.2
TS10	C_s	$^3A''$	−473.775 85	2.062	−9.09	−93.69	−8.65	11.07	−8.72	−473.916 35	−10.1
TS11	C_s	$^2A''$	−473.200 85	0.769	−12.69	−99.71	−4.83	7.98	−9.53	−473.349 82	+164.6[e]

[a]In a.u.
[b]For the HF/6-311G(d,p) wave function.
[c]Component of G2 energy in 10^{-3} a.u. For triplet species of stoichiometry H_2SO $n_{pair}=6$ and $n_{unpair}=2$, so that $\Delta E(HLC)=-0.037\,22$ a.u. For species of stoichiometry HSO $n_{pair}=6$ and $n_{unpair}=1$, so that $\Delta E(HLC)=-0.037\,03$ a.u.
[d]Enthalpy relative to $O(^3P)+H_2S$ at 0 K, in kJ mol^{-1}.
[e]For this species plus an H atom.$SrTiO_3$

along the reaction coordinate, HSO is always formed with at least some internal excitation. Then E_{tot} would underestimate the product energy, and the derived ΔH_0 and thus $\Delta H_{f,0}$(HSO) would be too positive. We hope in the future to test this interpretation by trajectory simulations on the PES outlined below. The present work may also be compared to data from previous theoretical investigations summarized in Table I. Our results are in close accord with those of Xantheas and Dunning[37] and Esseffar *et al.*,[44] but earlier *ab initio* calculations performed poorly and incorrectly yielded HOS as the more stable isomer. Xantheas and Dunning[37] attributed this to three deficiencies: (a) failure to account for nondynamical correlation, (b) lack of high angular momentum basis functions, and (c) poor geometries for HOS and HSO, which are seen to be overcome at the approximate QCISD(T)/6-311+G(3df,2p)//MP2=FULL/6-31G(d) level used here.

Our enthalpies for HSO and HOS, combined with other heats of formation,[56] yield the following bond dissociation enthalpies at 0 K, DH_0: H–SO, 240.0, H–OS, 225.7, HS–O, 406.3, and HO–S, 315.8 kJ mol^{-1}. The H–O bond strength in HOS is therefore considerably reduced from the 493.3 kJ mol^{-1} found for H_2O and 350.8 kJ mol^{-1} found for H_2O_2,[56] and the H–S bond strength is lowered from DH_0(S–H)=376.1 kJ mol^{-1} in H_2S.[56,61] The data in Table V lead[56,61] to calculated enthalpy changes for $HSO+O_3 \rightarrow HS+2\ O_2$ of 14.2 and 20.2 kJ mol^{-1} at 0 and 298 K, respectively. Thus reaction (2b) is calculated to be significantly endothermic and may have a reduced role in atmospheric chemistry.

TABLE IV. Comparison between GAUSSIAN-2 and experimental thermochemistry for minima on the $O(^3P)+H_2S$ PES, in kJ mol^{-1}.

Species	GAUSSIAN-2 $\Delta H_{f,0}$	Experimental $\Delta H_{f,0}$	Refs.
$O+H_2S$	226.8	229.2±0.8	56
OH+SH	178.8	180.9±3.2	56,61
H_2O+S	31.0	35.8±0.3	56
H_2+SO	8.3	5.0±1.3	56
HOS+H	213.3	216.7±8.4[a]	38,56
HSO+H	199.0	209.3±2.9	22,56

[a]Data extrapolated to 0 K.

The G2 energies of *cis* and *trans* ^{3}HOSH at the MP2=FULL/6-31G(d) geometries are above that of OH+SH, but the MP2=FULL/6-31G(d) transition states between these species (TS6 and TS7), with extended S–O distances of around 2 Å, have *lower* energies at the G2 level and are bound by 22.5 and 13.2 kJ mol^{-1}. Apparently, the geometry optimizations seriously underestimate the S–O bond length, so these G2 binding estimates are lower limits. It does seem clear that there is a weakly bound triplet state of HOSH. Combination with the G2 energy for singlet HOSH[59] yields an adiabatic separation of $\leqslant$265 kJ mol^{-1} from the TS6 structure.

C. Kinetics

Figure 3 illustrates the vibrationally adiabatic PES at 0 K, based on G2 enthalpies relative to $O(^3P)+H_2S$. This diagram may be contrasted to Fig. 2, derived with a much smaller basis set and a lower level of correlation correction. The main qualitative difference is that the energies of several MP2=FULL/6-31G(d) transition states now fall unphysically *between* the reactants and products they connect. This is consistent with the idea that there is no barrier to these processes in the exothermic direction, and we predict close to gas-kinetic rate constants, of the order of 1×10^{-10} cm^3 molecule^{-1} s^{-1}, for reactions (5), (8), and (9). It should be noted that H can also react with HOS and HSO on a

TABLE V. Thermochemical data for HSO.

T (K)	C_p (J K^{-1} mol^{-1})	S (J K^{-1} mol^{-1})	H_T-H_0 (kJ mol^{-1})	ΔH_f^0 (kJ mol^{-1})	ΔG_f^0 (kJ mol^{-1})
200	33.7	227.4	6.7	−18.4	−27.9
298.15	35.7	241.2	10.0	−19.9	−32.2
400	38.6	252.1	13.8	−23.8	−36.1
500	41.4	261.0	17.8	−26.7	−38.8
700	45.8	275.7	26.6	−31.0	−42.9
1000	50.1	292.8	41.0	−87.5	−40.0
1300	52.7	306.3	56.5	−87.6	−25.7
2000	55.6	329.7	94.6	−87.7	7.6

singlet PES without barriers, as discussed elsewhere,[59] and form HOSH and/or H_2SO. There appears to be no barrier to formation of the triplet HOSH adduct discussed in Sec. III B from OH+HS although, because its weak bonding will give only a small equilibrium population of adduct, the pathway through TS5 is likely to dominate under most conditions. We find no channels from $O+H_2S$ to HOS or SO, i.e., reactions (1c) and (1d) do not appear to occur by a direct mechanism, although Fig. 3 shows several pathways to these products via secondary chemistry and these might be important, e.g., for combustion modeling. Further evidence against the occurrence of reaction (1d) in a single elementary step is that, within the rules of orbital correlation and with the assumption of a C_s "least symmetrical complex,"[65] the products $SO(^3\Sigma^-)$ and $H_2(^1\Sigma^+)$ can only correlate on a $^3A''$ surface and all such surfaces connecting $O(^3P)+H_2S$ are already accounted for by TS1 and TS2 i.e., the products do not correlate with ground-state reactants. Balucani *et al.* did not observe formation of SO in single-collision experiments carried out at collision energies of up to 49 kJ mol^{-1}.[66] We can also imagine a fifth exothermic channel

$$O(^3P)+H_2S\rightarrow S(^3P)+H_2O \tag{1e}$$

that might occur at very high collision energies, but did not locate a TS for this to occur by a direct mechanism. A low-barrier pathway to the same products involving OH+SH is shown on Fig. 3. No bound triplet "H_2SO" intermediate was found, contrary to the suggestion of Smardzewski and Lin[17] who saw formation of singlet HOSH in experiments carried out in a frozen Ar matrix. A reinterpretation of their observations is that OH and SH were initial products, and then in the frozen Ar cage combined to give bound triplet HOSH which, especially aided by possible interactions with the matrix, relaxed through intersystem crossing to the singlet ground state. OH+HS may also combine to form singlet HOSH directly and without a barrier, as we showed elsewhere.[59]

Grice and co-workers first characterized TS3,[45] but its energy is too high for it to have played any role in their beam experiments with collision energies of around 30 kJ mol^{-1}.[20] Results of our searches along the intrinsic reaction coordinate (IRC) are in agreement with their conclusion that as the O atom attacks H_2S on the $^3A'$ surface the geometry tends towards the planar geometry shown in Fig. 1 as TS4. Unfortunately, the IRC algorithm breaks down as this system approaches planarity. It is troubling to indicate two transition states without an intervening minimum and, further, IRC analysis of TS4 shows that it is in fact the TS for H-atom exchange such as

$$D+HSO\rightarrow H+DSO. \tag{13}$$

Thus the idea that TS4 describes reaction (1b) is not firmly supported.

TS1 and TS2 control $^3A''$ abstraction and ^3A displacement pathways, respectively. The geometry of TS1 is similar to that obtained by Takane and Fueno[46] at the HF/6-31G(d,p) level, but they assigned their TS as $^3A'$. We find, with their basis set and geometry,[46] that the lowest energy HF wave function is $^3A''$ and that the first $^3A'$ state is excited by 179 kJ mol^{-1} at the CIS/6-31G(d,p) level. Takane and Fueno[46] located a planar TS for displacement at the HF/6-31G(d,p) level while we find that inclusion of a correlation correction leads to a pyramidal structure (see Fig. 1), similar to the MP2=FULL/6-31G(d) geometries described by Chang and Loew[40] for the analogous processes $O+CH_3SH\rightarrow CH_3+HSO$ and $H+CH_3SO$. The G2 enthalpy barriers at 0 K, $E_0^{\ddagger}$, are much closer to the measured E_a than

TABLE VI. Thermochemical data for HOS.

T (K)	C_p (J K^{-1} mol^{-1})	S (J K^{-1} mol^{-1})	H_T-H_0 (kJ mol^{-1})	ΔH_f^0 (kJ mol^{-1})	ΔG_f^0 (kJ mol^{-1})
200	34.1	226.4	6.7	−4.1	−13.4
298.15	36.7	240.5	10.1	−5.5	−17.6
400	39.6	251.7	14.0	−9.3	−21.4
500	42.0	260.8	18.1	−12.1	−24.1
700	45.3	275.5	26.9	−16.4	−28.1
1000	48.6	292.3	41.0	−73.2	−25.1
1300	50.9	305.3	56.0	−73.8	−10.6
2000	54.2	328.0	92.9	−75.1	23.7

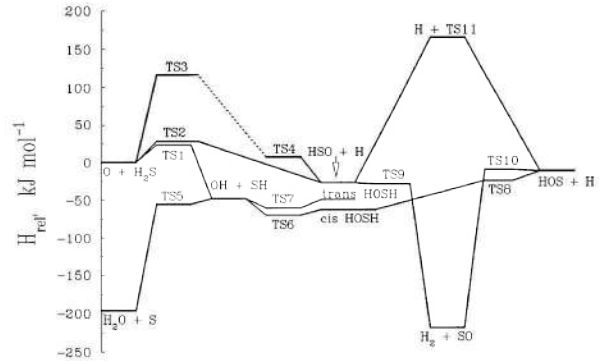

FIG. 3. Potential energy surface calculated at the G2 level, showing enthalpies at 0 K relative to $O(^3P)+H_2S$.

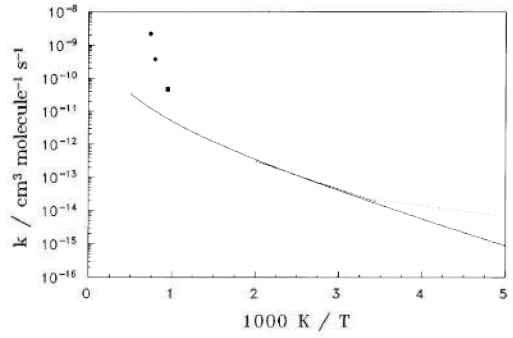

FIG. 4. Arrhenius plot for $O+H_2S$, showing TST fit for k_{1a} (solid curve), experimental recommendation of Ref. 3 (dashed line), data of Hollinden *et al.* Ref. 9 (dotted line), and flame measurements from Ref. 4 (●) and Ref. 5 (■).

previous values,[46] although of course $E_0^{\ddagger}$ is not equivalent to E_a. The slightly greater $E_0^{\ddagger}$ for TS2 is consistent with the observation that displacement of HSO accounts for at most 20% of the consumption of atomic oxygen.[16] The kinetics, branching ratio and isotope effects[58] are now considered in more detail by means of canonical transition state theory (TST):[67]

$$k_{\mathrm{TST}}=\Gamma l^{\ddagger}\frac{k_BT}{h}\frac{Q^{\ddagger}}{Q_O Q_{H_2S}}\exp\left(-\frac{E_0^{\ddagger}}{RT}\right). \tag{14}$$

Γ is a correction term for quantum mechanical tunneling, $l^{\ddagger}$ is the reaction path degeneracy and the Q's are the partition functions. Each Q is estimated from the MP2=FULL/6-31G(d) data with the usual assumption of separability of the vibrational and rotational motions. The experimental electronic partition function Q_{el} for $O(^3P_J)$ where $J=0$, 1 or 2 is $5+3\exp(-228\ \mathrm{K}/T)+\exp(-326\ \mathrm{K}/T)$,[56] Q_{el} for H_2S is 1, and a value of 3 was assumed for Q_{el} for each TS. In this way TS1, TS2, and TS3 account for the 9 states expected from $H_2S+O(^3P_J)$ interactions. Rotational symmetry factors were set equal to 1, and symmetry was taken into account via $l^{\ddagger}=2$. Γ is estimated in a simple way by means of the Wigner expression[68] based on the imaginary frequency for motion along the reaction coordinate, ν_i, calculated at the MP2=FULL/6-31G(d) level

$$\Gamma\approx 1-\frac{1}{24}\left(\frac{h\nu_i}{k_BT}\right)^2. \tag{15}$$

We do not expect this expression for Γ to be quantitatively accurate when tunneling is large.

Because abstraction is the dominant pathway,[15] we first test the accuracy of our kinetic analysis by fitting k_{1a}, derived via TST, to the experimental recommendation of Atkinson *et al.*[3] for the overall k_1 over 298–500 K with $E_0^{\ddagger}$(TS1) as the only adjustable parameter. This yields $E_0^{\ddagger}(\mathrm{TS1}) = 19.8\ \mathrm{kJ\ mol^{-1}}$, in excellent accord with the G2 value of 23.4 kJ mol^{-1}. Experiments indicate that k_1 is at least 80% attributable to this channel 1a at 298 K,[15] so that the worst error that arises from neglect of channel (1b) in this fit is only 0.6 kJ mol^{-1}. Figure 4 shows a comparison of the fitted TST rate constant with experimental data: agreement with the experimental recommendation[3] for 290–500 K is very good. The TST result over 200–2000 K may be summarized to within 6% as $k_{1a}=1.24\times10^{-16}(T/\mathrm{K})^{1.746}\exp(-1457\ \mathrm{K}/T)$ cm^3 molecule^{-1} s^{-1}. Also shown on Fig. 4 are results from flame measurements[4,5] which appear to be significantly too high, as are the low temperature measurements of Hollinden *et al.*[9] It is especially hard to measure small rate constants reliably, and the latter work may have been influenced by unsuspected secondary chemistry.

The branching ratio k_{1b}/k_{1a} is of interest, as outlined in Sec. I. TS2 for (1b) is tighter than TS1 for (1a), which leads to a smaller predicted pre-exponential A factor for the displacement channel: linear Arrhenius fits to the TST rate constants over 298–500 K yield $A=2.9\times10^{-12}$ cm^3 molecule^{-1} s^{-1} for k_{1b} and $A=2.0\times10^{-11}$ cm^3 molecule^{-1} s^{-1} for k_{1a}. Based on the G2 barriers, the predicted branching ratio varies from about 0.01 at room temperature to 0.06 at 2000 K, and is shown on Fig. 5. While these values are consistent with the limited experimental data, it should be noted that the k_{1b}/k_{1a} is sensitive to any errors in the quantity $E_0^{\ddagger}(\mathrm{TS1}) - E_0^{\ddagger}(\mathrm{TS2})$ and even one precise measurement of the branching ratio would permit reliable extrapolation over a wide range of temperature. In this context we note that the single-collision experiments of Davidson *et al.*[20] and Balucani *et al.*[22] yielded different

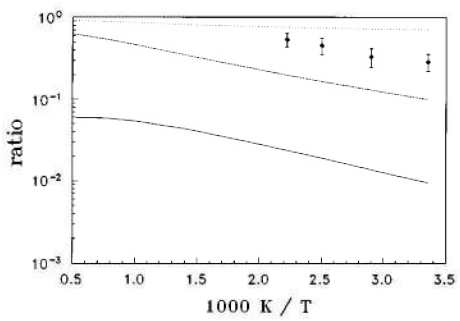

FIG. 5. Ratios of (1) TST rate constant for $O+H_2S\rightarrow HSO+H$ relative to $O+H_2S\rightarrow OH+HS$ (solid line), (2) $O+D_2S\rightarrow OD+DS$ relative to $O+H_2S\rightarrow OH+HS$ (dashed line), (3) $O+D_2S\rightarrow DSO+D$ relative to $O+D_2S\rightarrow OD+DS$ (dotted line), and (4) experimental overall rate constant for $O+D_2S$ relative to $O+H_2S$ Ref. 11 (●).

translational energy thresholds for reaction (1b) of 14±2 and about 25 kJ mol^{-1}, respectively. While a threshold is not identical to $E_0^{\ddagger}$, if the former value is correct then the ratio of k_{1b} to the TST value for k_{1a} would be considerably increased.

Figure 5 also illustrates the effects of deuterium substitution on reaction 1. A significant amount of ZPE is lost in going from reactants to TS1 and, as the deuterated species have lower frequencies,[69] $E_0^{\ddagger}$(TS1) is 3.5 kJ mol^{-1} higher for $O+D_2S$ than for $O+H_2S$. ν_i is reduced by close to a factor of $\sqrt{2}$, which reduces Γ, and both effects contribute to a large predicted kinetic isotope effect (KIE). Even if tunneling is neglected completely, k_{1a} for H_2S is still calculated to be about 6 times greater than k_{1a} for D_2S at room temperature. Note that these KIEs are independent of the magnitude of $E_0^{\ddagger}$. The properties of TS2 cause a quite different KIE for the displacement channel. In this case ν_i is small and varies little with deuteration,[69] and the ZPE of reactants and TS are similar both for H_2S and D_2S, with the result that k_{1b} is nearly unchanged. The experimental KIE obtained by Whytock *et al.*[11] falls midway between the KIEs predicted for the two channels: this perhaps suggests that both channels might be significant, contrary to the work of Singleton *et al.*[16] More experiments would certainly be helpful.

TST yields a rate constant expression for reaction 10 of $k_{10} \approx 2.97\times10^{-17}\ (T/\mathrm{K})^{1.94}\ \exp(-800\mathrm{K}/T)$ cm^3 molecule^{-1} s^{-1} for $T=298-2000$ K. There is a very weak temperature dependence, that reflects the small G2 $E_0^{\ddagger}$ of 3.5 kJ mol^{-1}. As argued above, $k_9 \approx 10^{-10}$ cm^3 molecule^{-1} s^{-1}, so that although H is more strongly bound in HSO than in HOS, it may be slightly more labile with respect to H-atom attack.

The DH_0(H–SO) and DH_0(H–OS) values in Section III B represent lower limits to the energy barriers for dissociation of HSO and HOS; Xantheas and Dunning[37] found no further barrier for HSO but an extra 10.0 kJ mol^{-1} barrier beyond the endothermicity for HOS. Thus the lowest energy unimolecular process for both HSO and HOS is isomerization, controlled by TS11 whose G2 energy is 192.4 kJ mol^{-1} above HSO. The geometry in Fig. 1 and vibrational frequencies in Table II are significantly different from earlier HF[36] and CASSCF+1+2[37] results, although the CASSCF+1+2[37] $E_0^{\ddagger}$ of 193.7 kJ mol^{-1} and the G2 value are in excellent accord. The kinetics of isomerization of HSO to HOS are analyzed in terms of RRKM theory as outlined by Gilbert and co-workers.[70,71] Rate constants are derived for an Ar bath gas, on the assumption of a weak collision "exponential down" model for energy transfer between the bath gas and HSO. $\sigma=3.66$ Å and $\epsilon/k_B=202$ K were chosen as the Lennard-Jones parameters that describe Ar+HSO collisions, based on suggested values for SO and the similarity between parameters for HO_2 and O_2.[72] Angular momentum effects for the molecule and TS11 are taken into account by allowing the energy of the rotational mode with the greatest moment of inertia to be active,[70] i.e., to be available to help cross the potential barrier, while the other two rotations were taken to be inactive. The kinetic results were multiplied by the tunneling factor Γ discussed above; the effect is to increase rate constants by a factor of 2.3 at 750 K that decreases to 1.2 at 2000 K. Reaction (11) is found to be at or close to the low-pressure limit for $T>200$ K and pressures below 2.5×10^5 Pa. Figure 6 shows an Arrhenius plot of the second-order $k_{11,0}$ and the reverse low-pressure limiting rate constant $k_{-11,0}$. The high barrier makes reaction (11) slow, except under combustion conditions, so that HOS and HSO should be detectable separately.

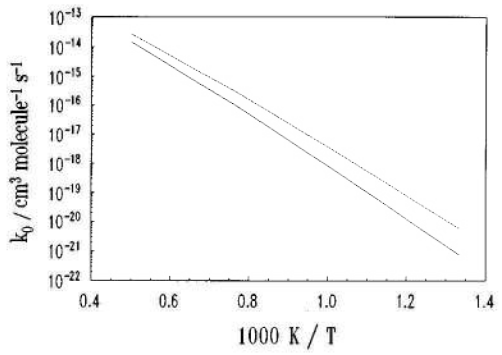

FIG. 6. Low-pressure limit RRKM rate constants k_0 for HSO→HOS (solid line) and reverse reaction (dashed line) in Ar bath gas.

IV. CONCLUSIONS

Structures and vibrational frequencies for minima and 11 transition states on the $O(^3P)+H_2S$ potential energy surface have been characterized at the MP2=FULL/6-31G(d) level. Experimental data are available for HSO and the theoretical results are in good accord. GAUSSIAN-2 theory was employed to calculate the thermochemistry of HSO and HOS, and the results suggest the potentially important atmospheric reaction $HSO+O_3 \rightarrow HS+2\ O_2$ is endothermic. Comparisons with ΔH_f for known asymptotes on the PES gave excellent agreement, except in the case of HSO, for which a possible rationalization is given. The kinetics of HSO⇌HOS isomerization are analyzed by RRKM theory. Transition state theory analysis of $O+H_2S \rightarrow OH+HS$ shows good accord with experiment, and the energy barrier is well described by G2 theory. Kinetic isotope effects and the branching ratio for H+HSO production are also analyzed. The other possible products H_2+SO and H_2O+S do not appear to be formed in a single elementary step, but low-barrier pathways to these species via secondary reactions are identified. No bound adducts of $O+H_2S$ were found, but preliminary results for weakly bound triplet HOSH are presented.

Note added in proof. Very recent shock tube measurements on $O+H_2S$ by Tsuchiya *et al.*[73] confirm the accuracy of the TST fit for k_{1a}, and yield rate constants only 12% above theory at 1100 K and 5% above theory at 2000 K. Tsuchiya *et al.* modeled a complex set of secondary processes to obtain the branching ratio for HSO formation as 0.2±0.1 over 1520–1820 K, in reasonable accord with the prediction here of 0.06.

ACKNOWLEDGMENTS

J.-D.R.R. thanks the Ronald E. McNair Post-Baccalawreate Achievement Program for a scholarship. This work was supported by the Robert A. Welch Foundation

(Grant No. B-1174) and computer time was provided through the NSF Pittsburgh Supercomputing Center (Grant No. CHE900059P) and the UNT Faculty Research Fund.

[1] M. Frenklach, J. H. Lee, J. N. White, and W. C. Gardiner, Jr., Combust. Flame. **41**, 1 (1981).
[2] W. B. DeMore, S. P. Sander, D. M. Golden, R. F. Hampson, M. J. Kurylo, C. J. Howard, A. R. Ravishankara, C. E. Kolb, and M. J. Molina, *Chemical Kinetics and Photochemical Data for Use in Stratospheric Modeling*, Evaluation Number 10 (JPL, Pasadena, 1992), Publication No. 92-20.
[3] R. Atkinson, D. L. Baulch, R. A. Cox, R. F. Hampson, Jr., J. A. Kerr, and J. Troe, J. Phys. Chem. Ref. Data **21**, 1125 (1992).
[4] A. Levy and E. L. Merryman, Combust. Flame **9**, 229 (1965).
[5] E. L. Merryman and A. Levy, J. Air Pollution Control Assoc. **17**, 800 (1967).
[6] G. Liuti, S. Dondes and P. Harteck, J. Am. Chem. Soc. **88**, 3212 (1966).
[7] H. Niki and B. Weinstock, 15th Conference on Mass Spectrometry and Allied Topics, 1967 (unpublished), p. 337.
[8] L. T. Cupitt and G. P. Glass, Trans. Faraday Soc. **66**, 3007 (1970).
[9] G. A. Hollinden, M. J. Kurylo and R. B. Timmons, J. Phys. Chem. **74**, 988 (1970).
[10] S. Takahashi, Mem. Nat. Def. Acad. Jpn. **10**, 369 (1970).
[11] D. A. Whytock, R. B. Timmons, J. H. Lee, and J. V. Michael, J. Chem. Phys. **65**, 2052 (1976).
[12] I. R. Slagle, F. Baiocchi, and D. Gutman, J. Phys. Chem. **82**, 1333 (1978).
[13] D. L. Singleton, R. S. Irwin, W. S. Nip, and R. J. Cvetanović, J. Phys. Chem. **83**, 2195 (1979).
[14] D. L. Baulch, D. D. Drysdale, J. Duxbury, and S. J. Grant, *Evaluated Kinetic Data for High Temperature Reactions* (Butterworths, London, 1976), Vol. 3.
[15] D. L. Singleton and R. J. Cvetanović, J. Phys. Chem. Ref. Data **17**, 1377 (1988).
[16] D. L. Singleton, G. Paraskevopoulos, and R. S. Irwin, J. Phys. Chem. **86**, 2605 (1982).
[17] R. R. Smardzewski and M. C. Lin, J. Chem. Phys. **66**, 3197 (1977).
[18] J. N. Bradley and D. C. Dobson, J. Chem. Phys. **46**, 2865 (1967).
[19] J. N. White and W. C. Gardiner, Jr., Chem. Phys. Lett. **58**, 470 (1978).
[20] F. E. Davidson, A. R. Clemo, G. L. Duncan, R. J. Browett, J. H. Hobson, and R. Grice, Mol. Phys. **46**, 33 (1982).
[21] N. Balucani, L. Beneventi, P. Casavecchia, D. Stranges, and G. G. Volpi, J. Chem. Phys. **94**, 8611 (1991).
[22] N. Balucani, P. Casavecchia, D. Stranges, and G. G. Volpi, Chem. Phys. Lett. **211**, 469 (1993).
[23] G. S. Tyndall and A. R. Ravishankara, Int. J. Chem. Kinet. **23**, 483 (1991).
[24] R. R. Friedl, W. H. Brune, and J. G. Anderson, J. Phys. Chem. **89**, 5505 (1985).
[25] U. Schurath, M. Weber, and K. H. Becker, J. Chem. Phys. **67**, 110 (1977).
[26] A. B. Sannigrahi, H. H. Thunemann, S. D. Peyerimhoff, and R. J. Buenker, Chem. Phys. **20**, 25 (1977).
[27] A. B. Sannigrahi, S. D. Peyerimhoff, and R. J. Buenker, Chem. Phys. **20**, 381 (1977).
[28] S. W. Benson, Chem. Rev. **78**, 23 (1978).
[29] A. Hinchliffe, J. Mol. Struct. **66**, 235 (1980).
[30] B. R. De and A. B. Sannigrahi, J. Comput. Chem. **1**, 334 (1980).
[31] M. Kakimoto, S. Saito, and E. Hirota, J. Mol. Spectrosc. **80**, 334 (1980).
[32] N. Ohashi, M. Kakimoto, S. Saito, and E. Hirota, J. Mol. Spectrosc. **84**, 204 (1980).
[33] R. J. Buenker, P. J. Bruna, and S. D. Peyerimhoff, Israel J. Chem. **19**, 309 (1980).
[34] T. J. Sears and A. R. W. McKellar, Mol. Phys. **49**, 25 (1983).
[35] B. T. Luke and A. D. McLean, J. Phys. Chem. **89**, 4592 (1985).
[36] P. L. M. Plummer, J. Chem. Phys. **92**, 6627 (1990).
[37] S. S. Xantheas and T. H. Dunning, Jr., J. Phys. Chem. **97**, 6616 (1993).
[38] R. A. J. O'Hair, C. H. DePuy, and V. M. Bierbaum, J. Phys. Chem. **97**, 7955 (1993).
[39] C. F. Melius (unpublished work).
[40] Y.-T. Chang and G. H. Loew, Chem. Phys. Lett. **205**, 543 (1993).
[41] J. Espinosa-Garcia and J. C. Corchado, Chem. Phys. Lett. **218**, 128 (1994).
[42] M. Iraqui, N. Goldberg and H. Schwarz, J. Phys. Chem. **98**, 2015 (1994).
[43] V. R. Morris and W. M. Jackson, Chem. Phys. Lett. **223**, 445 (1994).
[44] M. Esseffar, O. Mó, and M. Yáñez, J. Chem. Phys. **101**, 2175 (1994).
[45] Z. Z. Zhu, J. J. W. McDouall, D. J. Smith, and R. Grice, Chem. Phys. Lett. **188**, 520 (1992).
[46] S. Takane and T. Fueno, Bull. Chem. Soc. Jpn. **66**, 3633 (1993).
[47] J. A. Pople, M. Head-Gordon, D. J. Fox, K. Raghavachari, and L. A. Curtiss, J. Chem. Phys. **90**, 5622 (1989).
[48] L. A. Curtiss, C. Jones, G. W. Trucks, K. Raghavachari, and J. A. Pople, J. Chem. Phys. **93**, 2537 (1990).
[49] L. A. Curtiss, K. Raghavachari, G. W. Trucks, and J. A. Pople, J. Chem. Phys. **94**, 7221 (1991).
[50] W. J. Hehre, L. Radom, P. v. R. Schleyer, and J. A. Pople, *Ab Initio Molecular Orbital Theory* (Wiley, New York, 1986).
[51] J. B. Foresman and Æ. Frisch, *Exploring Chemistry with Electronic Structure Methods* (Gaussian, Pittsburgh, 1993).
[52] M. J. Frisch, M. Head-Gordon, G. W. Trucks, J. B. Foresman, H. B. Schlegel, K. Raghavachari, M. A. Robb, J. S. Binkley, C. Gonzalez, D. J. Defrees, D. J. Fox, R. A. Whiteside, R. Seeger, C. F. Melius, J. Baker, R. L. Martin, L. R. Kahn, J. J. P. Stewart, S. Topiol, and J. A. Pople, GAUSSIAN90 (Gaussian, Pittsburgh, 1990).
[53] M. J. Frisch, G. W. Trucks, M. Head-Gordon, P. M. W. Gill, M. W. Wong, J. B. Foresman, B. G. Johnson, H. B. Schlegel, M. A. Robb, E. S. Replogle, R. Gomperts, J. L. Andres, K. Raghavachari, J. S. Binkley, C. Gonzalez, R. L. Martin, D. J. Fox, D. J. DeFrees, J. Baker, J. J. P. Stewart, and J. A. Pople, GAUSSIAN92 (Gaussian, Pittsburgh, 1992).
[54] R. Seeger and J. A. Pople, J. Chem. Phys. **66**, 3045 (1977).
[55] D. Laakso, C. E. Smith, A. Goumri, J.-D. R. Rocha, and P. Marshall, Chem. Phys. Lett. **227**, 377 (1994).
[56] M. W. Chase Jr., C. A. Davies, J. R. Downey, Jr., D. J. Frurip, R. A. McDonald and A. N. Syverud, *JANAF Thermochemical Tables*, 3rd ed., [J. Phys. Chem. Ref. Data **14** Suppl. No. 1 (1985)].
[57] R. B. Kuczkowski, R. D. Suenram, and F. J. Lovas, J. Am. Chem. Soc. **103**, 2561 (1981).
[58] Frequencies for all deuterated molecules and transition states have been calculated, and may be obtained from the authors.
[59] A. Goumri, J.-D. R. Rocha, D. Laakso, C. E. Smith, and P. Marshall, J. Chem. Phys. (in press).
[60] N. Oliphant, M. E. Rosenkrantz, and D. D. Konowalow, Chem. Phys. Lett. **223**, 7 (1994).
[61] J. M. Nicovich, K. D. Kreutter, C. A. van Dijk, and P. H. Wine, J. Phys. Chem. **96**, 2518 (1992).
[62] S. Nourbakhsh, K. Norwood, H.-M. Yin, C.-L. Liao, and C. Y. Ng, J. Chem. Phys. **95**, 946 (1991).
[63] R. E. Continetti, B. A. Balko, and Y. T. Lee, Chem. Phys. Lett. **182**, 400 (1991).
[64] G. N. Lewis and M. Randall, *Thermodynamics*, 2nd ed., revised by K. S. Pitzer and L. Brewer (McGraw-Hill, New York, 1961), Chap. 27.
[65] K. E. Shuler, J. Chem. Phys. **21**, 624 (1953).
[66] N. Balucani, L. Beneventi, P. Casavecchia, D. Stranges, and G. G. Volpi, J. Chem. Phys. **94**, 8611 (1991).
[67] K. J. Laidler, *Theories of Chemical Reaction Rates* (McGraw-Hill, New York, 1969), Chaps. 4 and 5.
[68] M. F. R. Mulcahy, *Gas Kinetics* (Nelson, London, 1973).
[69] Scaled MP2=FULL/6-31G(d) vibrational frequencies for deuterated TS1 are 1739i, 191, 297, 523, 730, and 2010 and for deuterated TS2 are 389i, 294, 508, 884, 1341, and 1947, in cm^{-1}.
[70] R. G. Gilbert and S. C. Smith, *Theory of Unimolecular and Recombination Reactions* (Blackwell, Oxford, 1990).
[71] R. G. Gilbert, M. J. T. Jordan and S. C. Smith, UNIMOL program (see Ref. 70), 1990.
[72] R. J. McKee, G. Dixon-Lewis, J. Warnatz, M. E. Coltrin, and J. A. Miller, Sandia Report No. SAND86-8246, 1986.
[73] K. Tsuchiya, K. Yokoyama, H. Matsui, M. Oya, and G. Dupre, J. Phys. Chem. **98**, 8419 (1994).